5-2014

SYNTHESIS AND CHARACTERIZATION OF POLYMERIC MICELLE DELIVERY SYSTEM AS A DRUG AND

Justin Nice
Clemson University, jbn212@gmail.com

SYNTHESIS AND CHARACTERIZATION OF POLYMERIC MICELLE DELIVERY SYSTEM AS A DRUG AND GENE DELIVERY CARRIE TO TREAT TRAUMATIC BRAIN INJURY

A thesis
Presented to
the Graduate School of
Clemson University

In Partial Fulfillment
of the Requirements for the Degree
Master of Science
Bioengineering

---

by
Justin Nice
May 2014

Accepted by:
Jeoung Soo Lee, Committee Chair
Ken Webb
Naren Vyavahare

Abstract

Traumatic brain injury (TBI) is a leading cause of death and disability worldwide. There is currently no effective therapeutic for the treatment of TBI. Primary injury, from the initial injury, causes contusions and hemorrhaging at the site of impact. Diffuse damage is caused throughout the brain from the impact; this includes axonal injury, hypoxic brain damage, brain swelling and vascular injury. Brain damage continues as the secondary injury; which is characterized by hypoxia, hypotension, amino acid excitotoxicity and ionic imbalance. All of these conditions cause additional cell death and damage. Inflammation, brought about by reduced cyclic AMP levels is also seen post-injury. After injury, the glial scar and myelin produce neurite growth inhibitory molecules. There are several different types of myelin associated inhibitors expressed by oligodendrocytes; these interact with multiple types of neuron surface receptors triggering the RhoA cascade, which inhibits actin polymerization and neurite outgrowth. Chondroitin sulfate proteoglycans (CSPG) expressed on astrocytes also inhibits growth through the same RhoA pathway. Several strategies have elected to knockdown the RhoA gene or other genes involved in the growth inhibition pathway.

The objective of this work is to develop novel neuron-specific nanotherapeutics for combinatorial therapy of drug and small interfering RNA (siRNA) targeting both extrinsic and intrinsic barriers to neuroplasticity. This neuron-specific polymeric micelle nanotherapeutics will be designed as follows: First, a cell-type specific targeting moiety such as an antibody can be conjugated to the polymeric micelle nanoparticle surface to

deliver nanotherapeutics specifically to neurons. Second, RhoA siRNA, can be targeted to common intracellular signal transduction pathways for inhibitory molecules such as myelin and CSPGs. Third, a hydrophobic drug, a phosphodiesterase 4 inhibitor (rolipram) will be incorporated in the PgP micelle to increase intrinsic neuronal growth capacity by preventing injury-induced reductions in cAMP levels.

To achieve this goal, we synthesized amphiphilic block copolymers, poly (lactide-co-glycolide)-graft-polyethylenimine (PLGA-g-PEI: PgP) using PLGA as a hydrophobic core forming block and PEI as a hydrophilic shell forming block and characterized the physico-chemical properties of the PgP micelle as a delivery carrier for combinatorial therapy of nucleic acid and drug. We demonstrated that the PgP micelle is a promising nucleic acid delivery carrier using phMGFP plasmid as a reporter gene in C6 (glioma) cells and primary chick forebrain neurons (CFN) cells in 10% serum containing media in vitro. We also studied incorporating rolipram in the PgP micelle and successfully conjugated an antibody (mouse IgG) on the surface of PgP. Currently, we are evaluating PgP as a siRNA delivery carrier to primary CFN cells and preparing PgP-mNgR1 using NgR1 monoclonal antibody and evaluating the feasibility of PgP-mNgR1 as a neuron-specific nucleic acid carrier for targeting neuron cells in a rat cortical neuron /astrocyte co-culture system. In the future, we will study rolipram-loaded PgP-Ab as a nucleic acid/drug carrier using RhoA siRNA in hypoxic conditions as a TBI model in vitro and a rat traumatic brain injury model in vivo.

Acknowledgments

I would like to acknowledge my research advisor Dr. Jeoung Soo Lee for her assistance and guidance. I would also like to thank my committee: Dr. Ken Webb and Dr. Vyavahare for their time and assistance. I also wish to thank my lab members Ben Green, Graham Temples and Dr. So Jung Gwak for their help. In addition I would like to thank past and current lab members of the MicroEnvironmental Engineering Laboratory for teaching me necessary techniques and allowing me to use their lab space. Additionally, I would like to thank Dr. Guzeliya Korneva for her assistance with HPLC/GPC, Dr. Pranjal Nahar for her assistance with hypoxia and Cassie Gregory for her assistance with brain dissection. Finally, I would like to thank my funding sources an Institutional Development Award (IDeA) from the National Institute of General Medical Sciences of the National Institutes of Health under grant number P20GM103444.

Table of Contents

Table of Contents (Continued)

Page

List of Tables

Table Page

List of Figures

Chapter 1

Introduction

1.1 Traumatic Brain Injury

Traumatic brain injury (TBI) is caused by a blow to the head which disrupts normal brain function. It is the most common cause of death and disability in young people. [1] Each year around 1.7 million traumatic brain injuries occur. The most common causes of the trauma are falls, vehicle accidents, hitting another object (ex. children running into wall) and assault. [2] The degree of damage can range from mild to severe. A mild TBI is usually a concussion with full neurological recovery. Severe TBI is often characterized by a coma, which has several long term effects. These effects include loss of cognitive function and motor function, impairment of senses and emotional changes. The initial trauma, termed as primary injury, from the initial blow causes localized damages such as brain contusions and hemorrhaging. Diffuse damage also occurs such as axonal injury, hypoxic brain damage, brain swelling and vascular injury; however the secondary injury, which happens after the trauma, is the leading cause of in hospital deaths after TBI. [1,3]

Secondary injury is caused by an increase in intracranial pressure, decrease in cerebral perfusion and vasogenic fluid accumulation. The secondary injuries lead to hypoxemia and hypotension, all of which lead to neuronal damage and death. Damage is also done to the brain chemically. For example, after injury there is an ionic imbalance, oxidative damage and release of amino acids (ex. glutamine) which cause excitatory

damage. The damage done to the blood brain barrier allows the influx of cytokines and chemokines which causes inflammation. [4]

The post-injury remodeling creates an environment that inhibits neuron regrowth from occurring. The major inhibitory groups are myelin associated inhibitors (MAI) and chondroitin sulfate proteoglycans (CSPG) associated with the extracellular matrix. Three common MAIs Nogo, oligodendrocyte-myelin glycoprotein (OMgp) and myelin associated glycoprotein (MAG) inhibit neurite outgrowth They all bind to the cell surface Nogo-66 receptor (NgR1) causing activation of the Rho and Rac cascade; inhibiting both actin polymerization and neurite outgrowth. [5,6] Heavy inflammation is also seen in TBI, this is caused by injury induced decreases in cyclic AMP (cAMP) levels. cAMP is involved in the activation of protein kinase A (PKA) which phosphorylates cAMP-responsive element binding protein (CREB). CREB is important for transcription of survival genes. PKA also phosphorylates nuclear factor-κB which suppresses inflammatory cytokines. [7]

There have been several different approaches to treating the underlying causes of traumatic brain injury. One option for increasing cell survival and axon growth is the delivery of neurotrophins. Studies have used nerve growth factor (NGF), brain-derived neurotrophic factor (BDNF), neurotrophin-3 (NT-3), NT-4/5, glial cell-line derived neurotrophic factor (GDNF) and leukemia inhibitory factor (LIF). Some showed axon growth and neuron survival. [8] However, neurotrophins also cause additional systemic effects such as an immune response. [9]

Neurotrophins stimulate axon growth; however the inhibitory environment caused by the post-injury remodeling still exists. The glial scar helps create this inhibitory environment by expressing chondroitin sulfate and keratin. The glial scar may also inhibit diffusion of growth promoting molecules by creating a physical barrier to diffusion. CSPGs are upregulated by astrocytes after CNS injury. The effect on growth inhibition was tested by using a chondroitinase treatment and deletion of scar forming astrocytes. [10] The study used chondroitinase ABC enzyme (cABC) to digest the CSPG side chains on the astrocytes. This showed increased axon sprouting after brain injury. [11] Another group knocked down chondroitin polymerizing factor instead of treating with an enzyme. The advantage of this method is that CSPGs are continuously synthesized thus an enzyme treatment may not be sufficient due to short enzyme activity time *in vivo*. Another disadvantage of the cABC enzyme is that it may cause an immune response. [10]

The Rho kinase (ROCK) pathway controls CSPG mediated inhibition of growth but it is also involved with growth inhibition molecules expressed on myelin. [12] These inhibition molecules, mentioned above are OMpg, MAG and Nogo-A. These factors all bind strongly to the NgR1 receptor on the surface of neurons. A study which deleted NgR1 in mice showed less brain injury volume, better performance in motor function testing, increased neurogenesis and axon sprouting and increased growth associated protein-43 (GAP-43). [5] GAP-43 is expressed in areas of the brain with higher plasticity (ex. hippocampus). It is important in the forming of new connections between neurons. However, MAIs bind to receptors other than NgR1 such as lingo-1 and p75 (TROY). Another study showed increased functional recovery when deleting the three signaling

molecules (OMpg, MAG and Nogo-A). [13] However, the CSPG and NgR1 controlled pathways both involve the Rho kinase so several studies have used this to increase regrowth. In one study the cells were treated with Y27632 which inhibits ROCK. [12] The other study researchers knocked down p75, NgR1 and RhoA using siRNA to silence gene expression. [14]

1.2 Gene Delivery

Gene delivery uses either DNA or RNA to induce or silence production of a protein. However, *in vivo* delivery of a nucleic acid without a carrier has many challenges. This includes degradation by enzymes, serum protein aggregation, phagocytosis and charge repulsion from the cell membrane; both nucleic acids and cell membranes are negatively charged. [15] Thus a delivery vehicle is often used being categorized into viral and non-viral methods.

Viral delivery systems are advantageous because they have high transfection rates; disadvantages include mutagenesis, carcinogenesis and immune response. The most popular viruses chosen for gene delivery have been retrovirus and adenovirus. Retroviruses are made up of double stranded RNA which can also carry foreign DNA. Long-term gene expression is also seen with cells because the delivered gene integrates into the host chromosome. Adenoviruses are double stranded DNA viruses which can also carry foreign DNA. They produce high transfection efficiency with rare chromosome integration. They have, however received negative attention due to a death caused by severe immune response. [16]

Non-viral methods are made up of chemical and physical delivery methods. Popular chemical methods include cationic lipids and polymers and natural polymers such as chitosan. Physical delivery methods include gene guns, electroporation and microinjection. [17] Liposomes are made up of lipids which have a polar head group and can form either monolayers or bilayers. Lipoplexes are formed when polycationic liposomes are mixed with polyanionic nucleic acids. Lipoplexes protect the nucleic acid from degradation. Liposomes have shown good transfection *in vitro* in non-serum conditions however when tested in cell cultures with serum and *in vivo*, they show very low transfection efficiency. This is because the negative charges on serum proteins aggregate with liposomes. In the blood stream these large aggregates cannot reach the target cell because of red blood cell surface absorption or getting trapped in mucus lining and tight junctions of epithelial cells. [18] PEG-liposomes have also been used to increase circulation time by shielding the liposome. [19]

Polymer based delivery systems are also used in place of lipids. Cationic polymers are chosen to form polyplexes with nucleic acids. Branched polyethylenimine, (PEI 25kDa) is a cationic polymer which has shown high proficiency for endosomal escape and gene transfer into cells [20]. This property is important because if the polyplex is contained in the endosome, endosomal enzymes degrade it causing inefficient gene transfer. PEI has the ability to initiate the proton sponge effect leading to endosomal escape. At physiological pH the secondary amines on PEI are not protonated;however at endosomal pH (5.0-5.5) the secondary amines on the PEI become protonated because the pH is lower than the pKa. [19] The additional positive charges inside the endosome cause

a charge gradient across the membrane. Negative chlorine ions cross into the endosome due to this charge gradient. The increase in ions causes increased osmolarity in the endosome, thus water enters the endosome. The additional water causes the swelling and bursting of the endosome allowing escape into the cytosol. [18,21] Like lipids PEI has been PEGylated to reduce interactions with blood components [22]. In addition to PEI highly branched polymers called dendrimers have also been studies for nucleic acid delivery. Some examples of dendrimers used are polyamidoamines (PAMAM), polypropelenimine (PPI). [23]

Polymeric micelles are made up of amphiphilic molecules which self-assemble in aqueous solution. Micelles are made up of a block copolymer with a hydrophobic (ex. Poly-lactide) and hydrophilic polymer (ex. Polyethylene glycol). Polymeric micelles are able to have long circulation times if designed to be larger 42kDa but have a particle size smaller than 200nm. Being above 42kDa allows micelles to avoid glomular excretion. Micelles below 200nm avoid recognition by the reticuloendothelial system (RES). This system works by marking of foreign materials with complement proteins which then target the material for removal. [19]

1.3 Blood Brain Barrier

The blood brain barrier (BBB) is a major barrier to delivery of therapeutics to the brain. The composition of the extracellular fluid in the brain is controlled by what can pass through this barrier. The barrier is made of endothelial cells bound together by tight junctions. [17] Several options exist to overcome the BBB; lipophilic carriers such as

liposomes can be used for treatment of the CNS; this is because hydrophilic drugs cannot pass through the BBB. In addition, a prodrug which is uptaken by the brain can be used. If a lipophilic option cannot be used the drug can also be conjugated to a peptide which will cause it to be transported by endocytosis through the endothelial cells which make up the BBB. [24]

Chapter 2

Objectives

2.1 Project Objectives

The limitations of current treatment options for traumatic brain injury are that they only treat a single factor inhibiting neurite regrowth. As described earlier, there are several factors present in the post-injury remodeling cascade that inhibit regrowth. Recently, combination therapies, those which treat multiple factors preventing recovery, for TBI have sparked increasing interest from several national heath institutes. [25] Because no one treatment option will elicit a total recovery from a severe TBI, the objective of this project was to develop a combination siRNA and drug therapeutic.

2.2 Therapeutic Carrier Design

The path to this goal started with the synthesis and characterization of a polymeric micelle to be used in a combination therapy for the treatment of TBI. The polymeric micelle is to be used as a targeted genetic and drug delivery vehicle. (Fig. 2.1) Anti-NgR1 antibody will be conjugated to the micelle. NgR1 is mostly expressed in neurons, thus the micelles will be targeted toward neurons so the siRNA and rolipram will only affect neurons.[26] The gene to be knocked down is RhoA, as stated earlier this is involved in common pathway shared by several factors which inhibits axon growth. Finally the drug to be loaded is the phosphodiesterase IV inhibitor rolipram. Rolipram was found to

restore cAMP levels *in vivo*. [7,27] Rolipram is a hydrophobic drug thus can be loaded into the micelle core. [28]

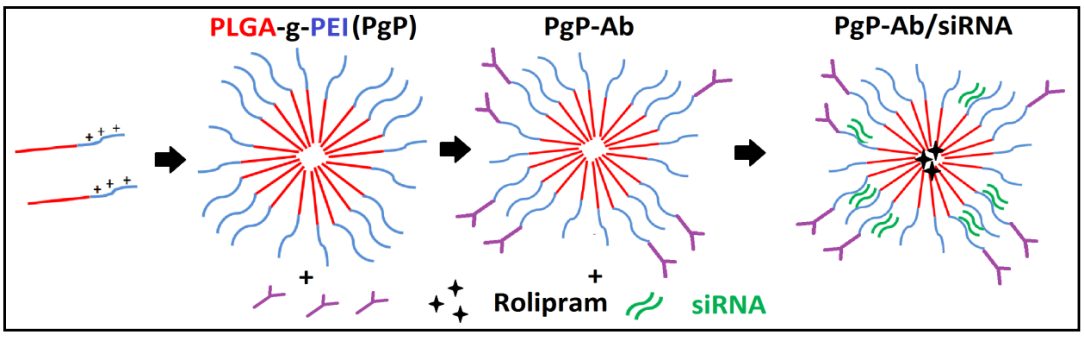

Figure 2.1 Micelle Scheme

Polymeric micelle nanoparticles are made from amphiphilic copolymers. Above a certain concentration in water, the critical micelle concentration, the polymer forms an ordered sphere. Due to thermodynamic instability of water interactions with a hydrophobic polymer the hydrophobic portions aggregate together in the micelle core. Likewise the hydrophilic portions point outwards. [29] Thus in order to form a micelle the polymer was designed with a hydrophobic and hydrophilic portion. Poly (Lactide-co-glycolide) (PLGA) a biocompatible, biodegradable hydrophobic copolymer was chosen as the hydrophobic portion of the polymer. [30] The hydrophilic portion of the micelle will consist of a polycation segment to form a polyplex with nucleic acids. [21] Branched PEI 25kDa as described above has high proficiency for endosomal escape. PEI also has the ability to conjugate a targeting antibody. PEI has primary amines which can react with aldehyde groups on oxidized targeting antibodies to form a Schiff base.[31]Due to these properties PEI was chosen as, the hydrophilic portion of the polymer. To achieve

our goal, we synthesized Poly (Lactide-co-Glycolide) –graft-Polyethylenimine (PgP) and characterized the physical-chemical properties.

2.3 Experimental Design

Three different PgPs were synthesized with branched PEI 25kDa and three different molecular weights of PLGA (4kDa (lactide:glycolide 50:50), 25kDa (lactide:glycolide 75:25) and 50k (lactide:glycolide 50:50)). A designation was given to each PgP based on the total PLGA composition. For example, "PgP-12k" is made up of 12kDa of PLGA (3 PLGA 4kDa:1 PEI), "PgP-25k" has 25kDa of PLGA per molecule (1 PLGA 25kDa:1PEI) and "PgP-50k has 50kDa of PLGA per molecule (1 PLGA 50kDA:1PEI). Particle size was used to determine micelle size and pDNA loading ability. Zeta potential and gel retardation were used to determine pDNA charge neutralization. N/P ratio is used in place of weight/weight ratio because the positive nitrogen groups on the polymer are what will bind to the negative phosphate groups on the nucleic acid. [32]

In order to test the ability of PgP to deliver nucleic acids, phMGFP (plasmid encoding human monster green fluorescent protein pGFP) was used as a reporter gene. Transfections were performed at various nitrogen/phosphate (N/P) ratios. PEI 5/1 was used as a positive control because it was previously shown to be the best cationic polymer for gene delivery. [33] Transfections were done in non-serum conditions and serum conditions. Serum conditions were used to more closely mimic *in vivo* conditions. Non-serum conditions were used as controls to test if PEI neutralization by the negatively charged serum proteins in serum conditions would cause lower transfection efficiency.

The hydrophobic drug rolipram was mixed with PgP to determine loading capacity. To conjugate the antibody to PgP, mouse IgG was oxidized by sodium periodate and then reacted with the primary amine of PEI in PgP micelles. The effect of antibody conjugation on transfection efficiency was also tested. To test the effect of Rolipram loaded PgP on neuronal survival; we used cobalt chloride $CoCl_2$ induced hypoxia as a model for traumatic brain injury.

Chapter 3

Materials and Methods

3.1 Materials

Poly (lactic-co-glycolic acid) (PLGA) (4kDa; 50:50, 25kDa; 50:50, and 50 kDa; 75:25) were purchased from Durect Corporation (Cupertino, CA). Anhydrous dimethylformamide (DMF), N-hydroxysuccidimide (NHS), dicyclocarbodiimide (DCC), branched polyethylenimine 25kDa (PEI), deuterium oxide (D_2O), sodium periodate, thiazolyl blue tetrazolium bromide (TBST), 2-mercaptoethanol, methanol, bromophenol blue, poly-L-lysine (PLL), acetonitrile (ACN), DNaseI and cobalt chloride hexahydrate were obtained from Sigma-Aldrich (St. Louis, MO). Dialysis tubing (MWCO: 50kDa, 300kDa) were obtained from Spectrum labs (Rancho Dominguez, CA). Unconjugated mouse IgG was obtained from Rockland Antibodies and Assays (Gilbertsville, PA). Sodium acetate and paraformaldehyde were purchased from Alfa Asesar (Ward Hill, MA). Bicinchoninic acid assay (BCA), bovine growth serum (BGS), Fetal bovine serum (FBS), DMEM/F12 50:50, Dimethyl sulfoxide (DMSO), tris-HCl, tris Base, sodium dodecyl sulfate (SDS), nitrocellulose membranes, D-glucose, sodium chloride, potassium chloride, potassium phosphate, sodium phosphate, penicillin, 1% trypsin, 0.25% trypsin and glycine were obtained from Thermo Fisher Scientific (Waltham, MA). Polyvinylidene fluoride (PVDF) membranes, Bis-acrylamide, Kaleidoscope ladder, Ammonium Persulfate and Tetramethylethylenediamine (TEMED) were purchased from Bio-Rad (Hercules, CA). WesternBreeze with anti-mouse secondary, basal medium eagle

(BME), trypsin/EDTA 0.05%, Alexa fluor secondary antibodies and 200mM L-glutamine were obtained from Life Technologies (Grand Island, NY). C6 cells were obtained from ATCC (Manassas, VA). Anti-HIF1α was obtained from Millipore (Billerica, MA). Anti-βIII tubulin and anti-β-actin antibodies were obtained from Abcam (Cambridge, MA). Rolipram was purchased from LC Labs (Woburn, MA). The C18 Column was obtained from Shodex (New York, NY). The Waters 1525 binary HPLC pump, Waters 2998 photodiode array detector, Waters 2414 refractive index detector and Ultrahydrogel 250 column were obtained from Waters (Milford, MA). The 90Plus Particle Size Analyzer was from Brookhaven Instruments Corporation (Holtsville, NY)

3.2 Synthesis of PgP

3.2.1 Synthesis of PgP

To synthesize PgP-12k, PgP-25k, and PgP-50k, the carboxylic end group on the PLGA (MW: 4kDa, 25kDa or 50kDa) was activated by NHS and DCC for two hours in DMF. PgP-12k was synthesized by using a 4:1 mole ratio of PLGA-4kDa to PEI and PgP-25k and PgP-50k were synthesized by using a 1.2:1mole ratio of PLGA-25kDa and PgP-50kDa to PEI. After the reaction, the reactant solution was filtered to remove dicyclohexyl urea. Following filtration, the activated PLGA was reacted with branched PEI (MW: 25kDa) by adding it drop-wise and then the mixture was allowed to react for 24hrs at room temperature with stirring. Poly (lactide-co-glycolide)–g-poly (ethylenimine) (PLGA-g-PEI: **PgP**) was purified by dialysis against deionized water

using a membrane filter (MWCO=50,000), filtered with a 0.2μm filter to remove the precipitate, and then freeze-dried.

Following synthesis and purification, the structure was verified by ^{1}H- NMR on a Bruker 300MHz in D_2O. The gel permeation chromatography (GPC) was carried out with a Waters 1525 binary high performance liquid chromatography (HPLC) pump and Waters 2414 refractive index detector. The mobile phase was Millipore water at a flow rate of 0.7mL/min. Injection volume was 20μL and run time was 15 minutes. The standards used were dextran at molecular weights of 5, 12, 25, 50 and 80kDa.Critical micelle concentration (CMC) was determined using dye dissolution. 10μL of 0.4mM 1,6 diphenyl- 1,3,5-hexatriene was added to 1mL PgP solutions at various concentrations. The solutions were incubated in the dark for 6 hrs. Absorbance was taken at 356nm and used to calculate CMC.

3.2.2 Antibody Conjugation

Antibody conjugation using mouse IgG was accomplished by first oxidizing the antibody with sodium periodate in isotonic sodium acetate buffer for 2 hours at 4^{o}C. The reaction was then terminated with ethylene glycol and dialyzed against sodium acetate once and against isotonic PBS twice to remove excess ethylene glycol and sodium periodate. [36] Protein concentration was then determined by BCA assay. PgP-12k was mixed with oxidized antibody to make a 40mg/mL PgP solution with a 50:1 ratio of PgP to antibody. The solution was mixed overnight at 4^{o}C and then dialyzed 24 hours against water (300kDa membrane) to remove unconjugated IgG. Antibody conjugation was

verified by immunoblot assay. A nitrocellulose membrane was washed with tris buffered saline (TBS) and then dried. Following drying 2µL dots of undialyzed PgP-IgG, dialyzed PgP-IgG, IgG standards and PgP were spotted on the paper and allowed to dry. Next the procedure included with the WesternBreeze kit was followed but the primary antibody step was omitted because the alkaline phosphates secondary antibody (anti-mouse) recognizes the mouse IgG directly. [37]

3.3 Characterization of PgP/pDNA Polyplexes

3.3.1 Particle Size and Zeta Potential

The particle size and zeta potential of PgP/pDNA polyplexes were determined by using Brookhaven Instruments Corporation 90Plus Particle Size Analyzer. PgP/pGFP complexes were prepared at various N/P ratios; PgP was mixed with pGFP (20µg) and incubated for 30 minutes at 37^{o}C. The solution was transferred to a 2mL cuvette and the particle size was measured. Particle size was measured three times for two minutes each using an angle of 90^{o} and wavelength of 659nm. Following particle size measurements, 1.7mL of solution was transferred to a new cuvette and the zeta potential electrode was inserted into the cuvette. Zeta potential measurements were taken three times.

3.3.2 Gel Retardation

A gel retardation assay was done to determine if DNA was completely complexed with PgP. 100µL of PgP/pGFP complexes were prepared at various N/P ratios by mixing PgP with pGFP and incubating for 30 minutes at 37^{o}C. The agarose gel was

prepared at 1% with an ethidum bromide concentration of 0.5μg/mL. 10μL of complexes were mixed with 3μL of loading dye. 10μL of sample was then loaded into each well. The gel was run at 80V until the xylene cyanol (light blue) dye was 2/3 through the gel. The images were taken using an Alpha Innotech FlourChem SP imager set to UV transillumination.

3.4 Cell Culture

C6 rat glioma cells were cultured with DMEM/F12 media supplemented with 5% BGS and 1% antibiotics at 37°C in 5% CO_2. Cells were passaged every 2-3 days and were not kept above passage 10.

Chick forebrain neurons were isolated from day eight embryonic chicks (E8); chicken eggs obtained from Clemson University Poultry Center and incubated at 37°C with light rocking. Polystyrene culture plates were coated with PLL by adding 0.01% PLL solution onto the plates for at least 1 hour and then washing with DI water twice to remove unbound PLL. After removal of the membrane from the forebrain the brains were incubated in 0.25% trypsin for 5 minutes at 37°C. The trypsin was then aspirated and the brains were triturated and suspended in complete media. The neurons were plated at 1 million cells/mL. The neurons were cultured in BME supplemented with 10% FBS, 6mg/mL D-glucose, 2mM L-glutamine and 1% antibiotic at 37°C in 5% CO_2.

Rat cerebellar neurons were isolated from day 3 postnatal rats. Rat cerebellums were isolated and the membranes and blood vessels were removed. The cerebellum was then minced and trypsinized for 15 minutes at 37°C in 1mL of 1% trypsin supplemented

with 100uL of 1% DNase. The solution was then centrifuged for 3 minutes at 1000 RPM. Next the trypsin was aspirated and the brains were resuspended in 5mL media and triturated. The neurons were further homogenized with a 3mL syringe with 22Gx1½ needle. Neurons were cultured on PLL plates as described previously at a concentration of 1 million cells/mL. [38] The culture medium used was BME supplemented with 10% FBS, 6 mg/mL D-glucose, 1.5 mg/mL KCl, 2mM L-glutamine and 1% antibiotic at 37^{o}C in 5% CO_2.

3.5 Transfection Efficiency and Cytotoxicity

PgP nucleic acid delivery capability was tested using transfection with phMGFP (pGFP) as a reporter gene. C6 cells were seeded at 1e5 cells/mL in 12 well plates. Plating media consisted of DMEM/F12 supplemented with 10% FBS and 1% antibiotic. Media for transfection was either serum containing or serum free depending on conditions desired. 24 hours after plating PgP/pGFP complexes were prepared at various N/P ratios on a basis of 2ug of pDNA and 100µL of volume per well. The complexes were well mixed and incubated for 30 minutes at 37^{o}C. For non-serum conditions, cells were washed and replaced with serum-free media. After incubation, the complexes were distributed drop-wise into each well. Four hours after transfection, cells were washed twice and replaced with 10% serum media. For 10% serum conditions, cells were washed and replaced with 10% serum media. Complexes were then distributed in the same manner. 24 hours after transfection, cells were washed twice and replaced with 10%

serum media. 48 hours after transfection, analysis of cell viability and percent transfection were performed.

Percent transfection was calculated using flow cytometery on a Millipore easyCyte flow cytometer with guavaCyte software. The cells were washed with PBS without calcium and magnesium and trypsinized. The trypsin was neutralized with media containing serum and the cells were diluted to less than 500 cells/µL. Each sample was run until 5000 events were counted.

Cell viability testing was calculated using MTT assay; the media was removed and replaced with serum-free media then 240µL of 2mg/mL TBST solution in PBS with calcium and magnesium was added to each well drop-wise. The wells were incubated for 4 hours at 37^{o}C, the media was aspirated and the remaining formazan crystals were dissolved in 1mL DMSO. The absorbance of the solution was read at 570nm.

3.6 Generation of Hypoxia as an *in vitro* TBI Model

Hypoxia was induced by treating cells with 100µM, 150µM and 200µM $CoCl_2$ in PBS with calcium and magnesium for 20, 24 and 44 hours. C6 cells were plated at 3e5 cells/mL in 6 well plates. Rat cerebellar neurons were plated at 1 million cells/mL in 6 and 96 well plates. The next day the media was changed and the appropriate amount of $CoCl_2$ was added to each well. At the desired time points, the cells were lysed using 200uL of RIPA buffer in each well. Total protein was assessed using BCA assay. Polyacrylamide gels were cast with a 10% resolving gel. Samples were diluted with reducing sample buffer so that 30µg of total protein was added to each well. After

dilution the samples were heated for 5 minutes at 60°C. The gel was run at 100V until sample buffer reached the bottom of the gel. The proteins were transferred to a PVDF membrane by western blotting at 30V overnight at 4°C. Following transfer the membrane was stained according to the WesternBreeze protocol using chromogenic detection for both anti-HIFα and anti-β-actin. Immunocytochemistry was done on rat cerebellar neurons with βIII-tubulin to detect morphological changes.

3.7 Rolipram Loading

Three separate variables were tested for their effect on rolipram loading. Rolipram amount added to PgP solutions, PgP solution concentration and PgP composition were tested. PgP-12k, PgP-25k and PgP-50k were used to measure rolipram loading efficiency with an increase hydrophobic core size. Amount of rolipram was tested by adding 1, 2 or 4mg to PgP to test if supersaturating with drug increased loading amount. Finally, concentration of PgP solution was tested using 1, 5 or 10mg/mL of PgP solution. The variables were all tested in parallel; there were three conditions for each of the three variables yielding 27 different conditions. Rolipram in amounts of 1, 2 or 4mg was dissolved in PgP 12k, 25k or 50k solutions at concentrations of 1, 5 or 10mg/mL, respectively. The samples were mixed while shaking for 6 hours at room temperature. The samples were then filtered with 0.2μm in preparation for HPLC. Reverse phase HPLC was used to determine rolipram loading. The HPLC was run on a Waters 1525 binary HPLC pump and detected with a Waters 2998 photodiode array detector set to 280nm. The column used was a Shodex C18. The mobile phase was 60:40 Millipore

water:ACN [28] Rolipram standards were dissolved in DMSO to make a standard curve of rolipram concentration. Injection volume was 20 µL and run time was 7 minutes. Each sample made in duplicate and injected twice.

Chapter 4

Results and Discussion

4.1 Synthesis of PgP

4.1.1 Synthesis of PgP

PgP was synthesized using branched polyethylenimine (b-PEI or PEI, MW 25 kDa) and three different MW of poly-D,L-(lactide-co-glycolide) (PLGA, MW 4 kDa, 25kDa, and 50kDa). Different molecular weights and ratios of lactide:glycolide were used to change the size of the hydrophobic core used for drug loading. Longer PLGA molecules were chosen to increase the hydrophobic tail length of the micelle. Higher lactic acid ratios were chosen to increase hydrophobicity of the polymer tail. Because there were three different PLGA molecular weights used, three different PgP molecules were synthesized. Following synthesis and purification, the structure and molecular weight (MW) of PgP was determined by ^{1}H NMR and GPC (Fig. 4.1 and 4.2). The structure of PgP was characterized by ^{1}H-NMR using D_2O as solvent (δ=2.4~3.5 (m, PEI backbone -CH_2), δ=1.4~1.6 (d, 3H, PLGA -CH_3), δ=4.3 (q, 1H, PLGA-CH), δ=3.9 (s, 2H, PLGA –CH_2)). The degree of PLGA graft to the PEI and molecular weight of PgP was calculated from the ratio of the integrals of the PEI back bone to methylene of PLGA (δ=3.9). In case of PgP-12k, approximately three 4 kDa of PLGA are grafted to one PEI and the molecular weight of PGP was calculated approximately 38,681Da by NMR and 38,168Da by GPC. In case of PgP-25k, approximately one of 25kDa of PLGA are

grafted to one PEI and the molecular weight of PgP was calculated approximately 49,275Da by NMR and 48,791Da by GPC (Table 4.1).

Critical micelle concentration (CMC) was calculated creating two linear fits to the concentration versus absorbance at 356nm. The logarithm of polymer concentration was plotted against absorbance. The graph shows a rapid spike at the critical micelle concentration. The intersection of the linear fit from the region before the rapid spike and after it is used to calculate the critical micelle concentration.

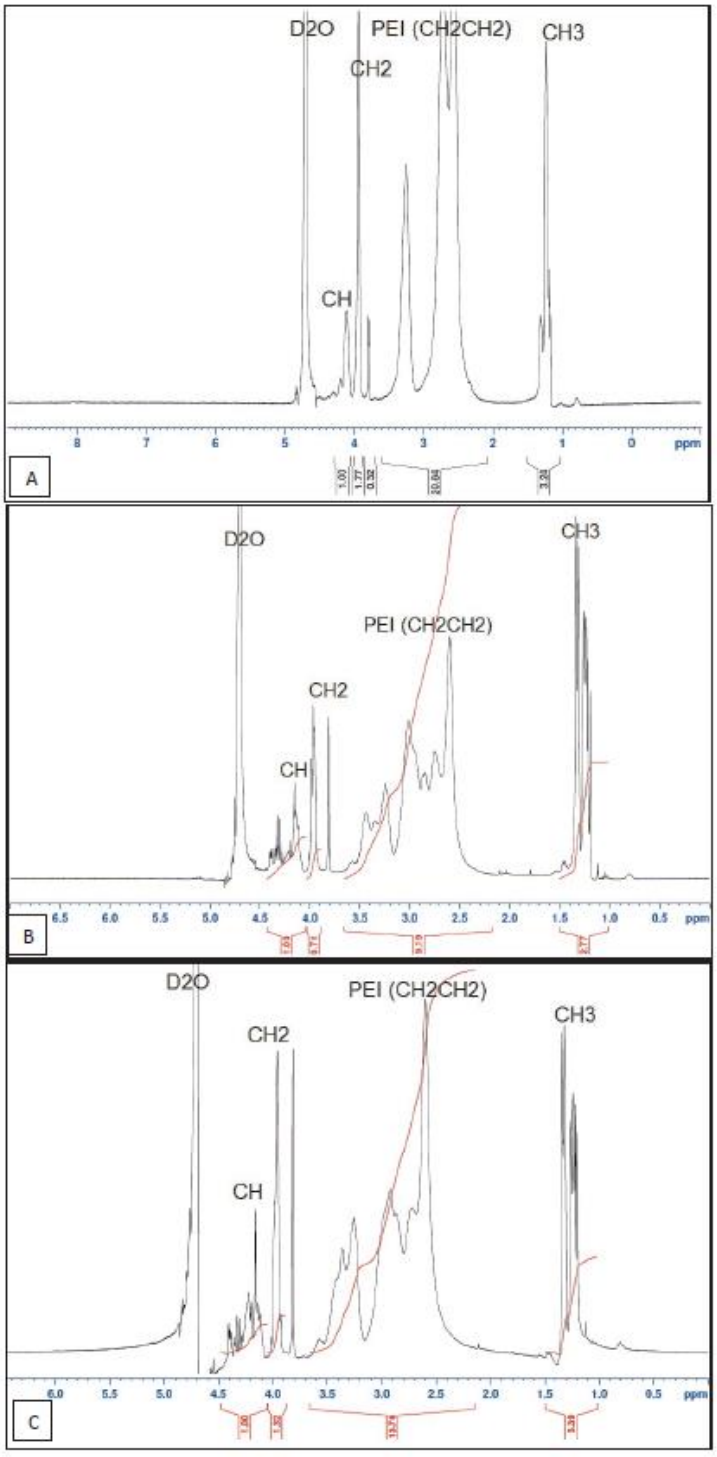

Figure 4.1 ^{1}H-NMR Spectra of PgP-12k (A), PgP-25k (B), PgP-50k (C)

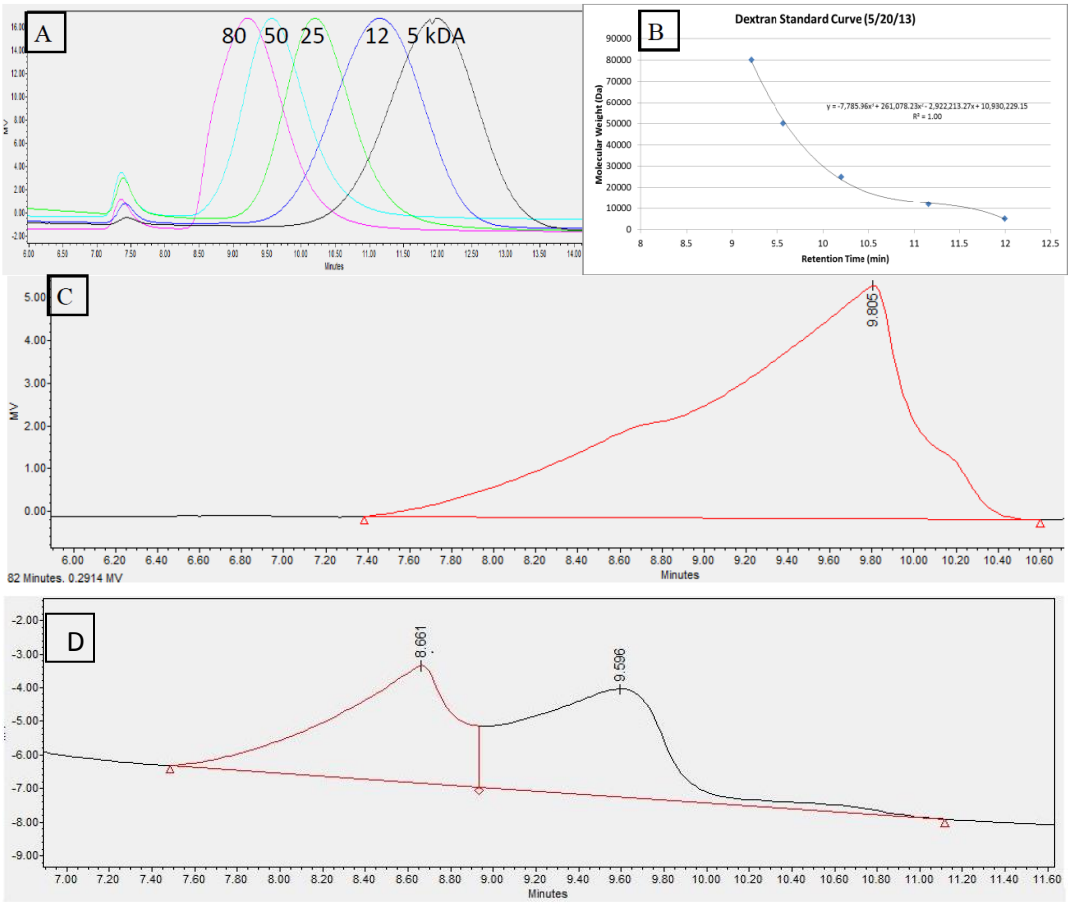

Figure 4.2 GPC of dextran standards (A), standard curve (B) PgP-12k (C) and PgP-25k (D)

	MW by NMR	MW by GPC	CMC (μM)
PgP-12k	38681	38168	18.6
PgP-25k	49275	48791	9.3

Table 4.1 NMR, GPC and CMC calculations for PgP at various molecular weights

4.1.2 Antibody Conjugation to PgP

Antibody conjugation with mouse IgG was verified by immunoblotting (Fig. 4.3). The density of colorimetric staining was used to compare undialyzed PgP-IgG to dialyzed PgP-IgG. The undialyzed PgP-IgG showed slightly greater colorimetric staining density compared to dialyzed PgP-IgG. The difference in colorimetric staining is attributed to oxidized IgG that was not conjugated to PgP and was thus removed by dialysis. PgP alone was also immunoblotted to check for background and none was seen.

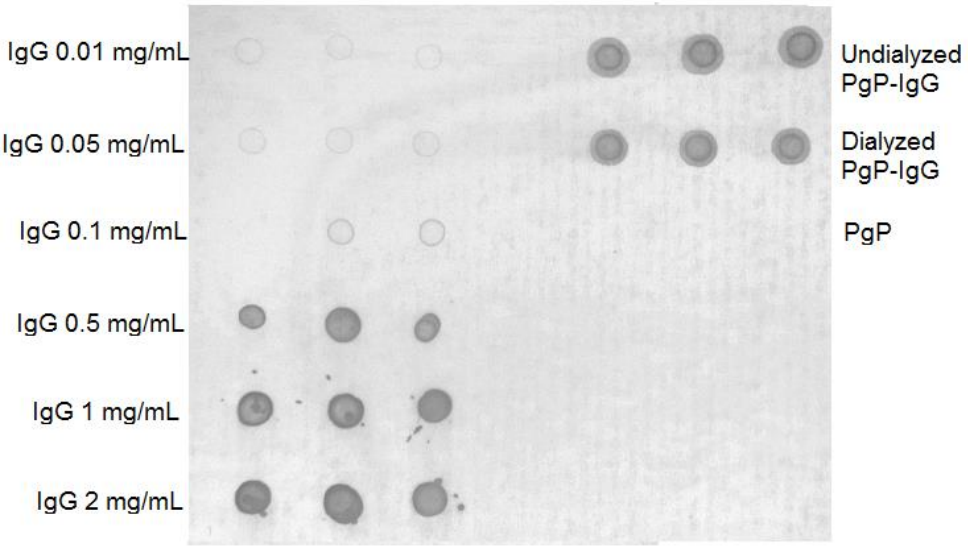

Figure 4.3 Immunoblot of 300kDa dialyzed PgP-IgG, undialyzed PgP-IgG, PgP and a serial dilution of IgG alone.

4.2 Characterization of PgP/pDNA Polyplexes

4.2.1 Particle Size and Zeta Potential

The particle size and zeta potentials were measured at various N/P ratios of PgP-12k/pGFP. Ratios above 2.5/1 completely neutralized the negative charge of the pDNA

by complexation with PgP. The particle size was found to be around 200nm. (Fig. 4.4A) The particle size and zeta potential were also taken for PgP-25k and PgP-50k. At w/w higher than 1/1 the pDNA was neutralized. The particle sizes were approximately 200nm and 150nm at all w/w ratios for PgP-25k and PgP-50k respectively. (Fig. 4.4B) The reason for the lower size with a higher molecular weight is most likely the larger hydrophobic core forming a tighter micelle. Based on this particle size data PgP-50k may be the best option for systemic injection *in vivo*. The reason for this is that particles above 200nm are subject for removal by the reticuloendothelial system [24].

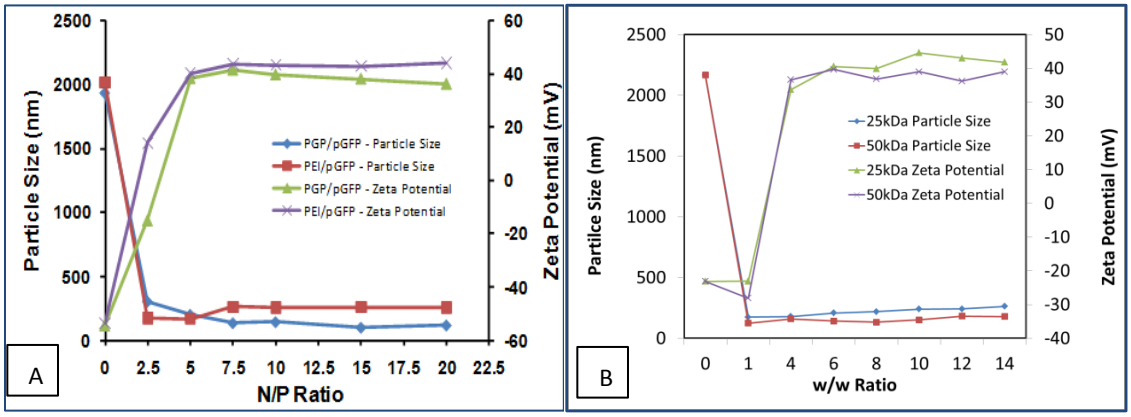

Figure 4.4 Particle size and Zeta Potential of PgP-12k, PEI (A), PgP-25k and PgP-50k (B)

4.2.2 Gel Retardation

Gel retardation was used to determine complex stability. PgP-12k at N/P ratios above 5/1 showed no pDNA migration, meaning the complex was completely stable. (Fig. 4.5A). For PgP-12kDa-Ab all w/w ratios used showed complete pDNA complex

formation (Fig. 4.5B). Weight/weight ratio was used because the exact amount of conjugated antibody was not known. N/P ratio could not be calculated because of this.

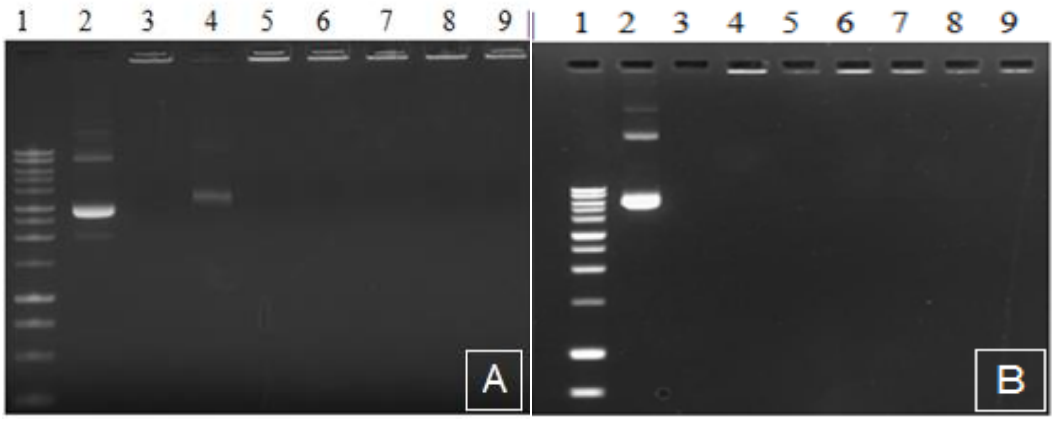

Figure 4.5 Gel retardation of PEI and PgP-12k (A) Lanes: 1 ladder, 2 pGFP, 3 PEI/pGFP N/P 5/1, 4-9 PgP-12k/pGFP N/P 5/1-30/1. Gel retardation of PEI and PgP-12k-Ab (B) Lanes: 1 ladder, 2 pGFP, 3 PEI/pGFP N/P 5/1, 4-9 PgP-12k-Ab/pGFP w/w 1/1-6/1

4.3 Transfection Efficiency and Cytotoxicity

First, transfection was done in non-serum conditions because serum severely inhibits transfection with the positive control PEI. In these conditions, higher ratios of PgP-12k showed a significant increase in percent transfection compared with PEI with no significant change in cell viability (Fig. 4.6A, B). Next, transfection was tested in 10% serum conditions because it more accurately mimics conditions seen *in vivo*. PEI performed as expected in serum conditions, with low transfection but PgP-12k showed increased percent transfection up to an N/P ratio of 30/1 with no decrease in cell viability (Fig. 4.6A, B). Representative images of C6 cells transfected with PgP-12k/pGFP show high levels of GFP expression with no change in cell morphology (Fig. 4.7). After

showing that PgP significantly outperforms PEI in serum conditions, non-serum conditions were no longer tested. PgP-25k and PgP-50k were tested with higher N/P ratios due to the higher molecular weights. PgP-25k showed higher transfection with lower cell viability (Fig. 4.6C, D). The same was true for PgP-50k (Fig. 4.6E, F). Transfection was also tested using PgP-12k-Ab. The percent transfection was higher than that of PgP-12k and PEI however the cytotoxicity was higher (Fig. 4.8A, B). All PgP transfections in C6 cells showed promising transfection results with much higher transfection than PEI and low to no cytotoxicity. Similar studies have transfected C6 cells with PEI based nanoparticles in non-serum and serum conditions with varying degrees of success. One study showed 25% percent transfection with 85% viability in C6 cells. [39] Another study showed 40% transfection with no cytotoxicity in serum conditions. [42] A targeting ligand based nanoparticle showed 60% transfection in serum conditions with no cytotoxicity. [43] Based on these studies our polymer is better than or on par with other transfections done in the same cell type. This is promising for future studies because we showed that our polymer has the ability to delivery nucleic acids to cells.

Transfection in CFN was done to show transfection capability in neurons. Non-serum transfection with PgP-12k showed similar percent transfection to PEI 5/1 with increased cytotoxicity at higher N/P ratios (Fig. 4.9A, B). Serum transfection with PgP-12k showed higher transfection than PEI 5/1 however it did show higher cytotoxicity. PgP-25k showed increased transfection with increasing N/P ratio with high toxicity (Fig. 4.9C, D). PgP-50k showed similar results (Fig. 4.9E, F). While the transfection percentage was not as high as in C6 cells it is known that non-dividing cells transfect at

much lower percentages than rapidly dividing ones when using a DNA based reporter. [41] Other studies have shown low rates of transfection in neurons with lipoplexes, around 4% hippocampal and cortical neurons. [40] Another showed similar results with branched PEI transfection in neurons. [44] Our polymer, showed its capability to deliver pDNA to neurons.

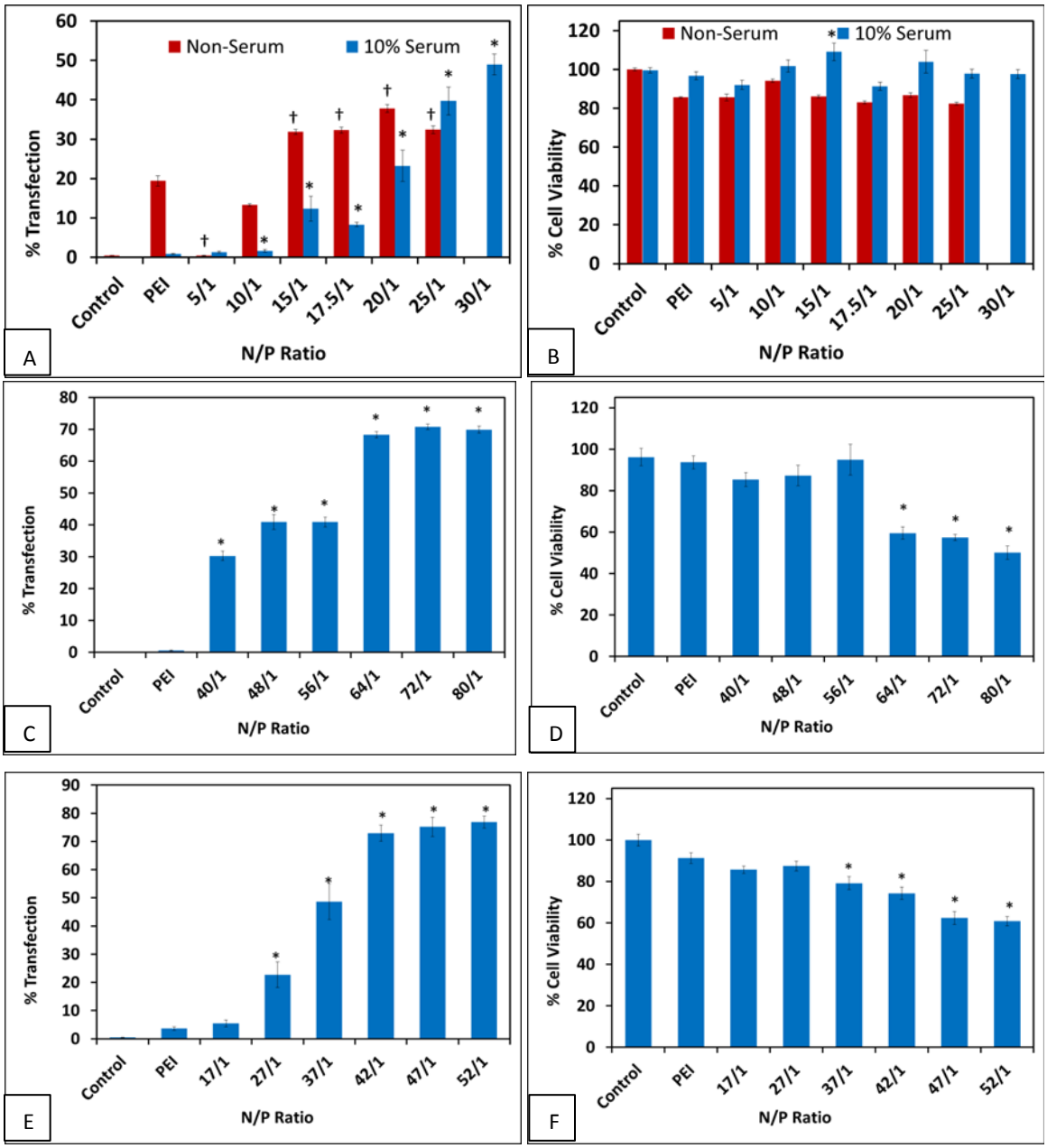

Figure 4.6 C6 cells transfected with PgP-12k/pGFP in 10% serum and non-serum conditions; percent transfection (A) and cell viability (B). C6 cells transfected with PgP-25k/pGFP in 10% serum; percent transfection (C) and cell viability (D). C6 cells transfected with PgP-25k/pGFP in 10% serum; percent transfection (E) and cell viability (F). PEI N/P is 5/1 *:P<0.05 for serum conditions, †:P<0.05 for non-serum compared to PEI

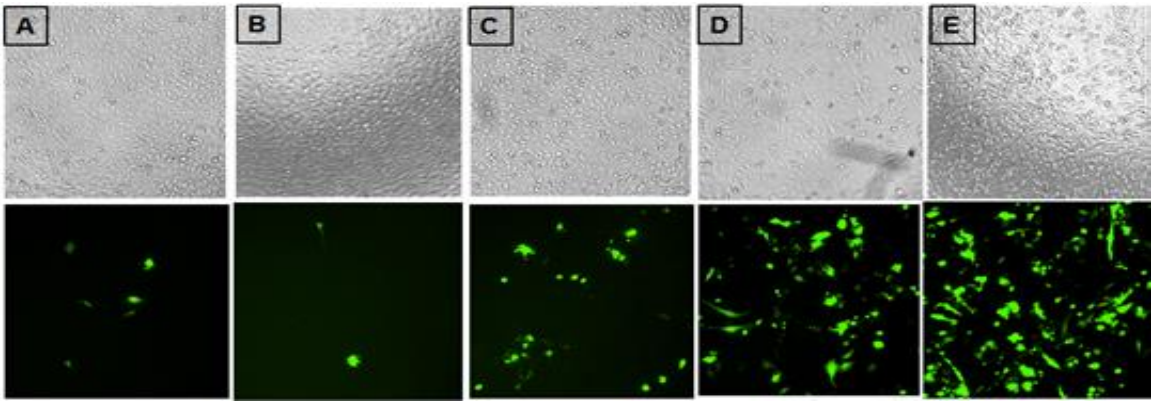

Figure 4.7 Representative images of transfected C6 cells. Magnification 100x, top: phase contrast, bottom GFP transfected cells. PEI/pGFP 5/1 (A), PgP-12k/pGFP 5/1, 10/1, 15/1 and 20/1 (B-E respectively)

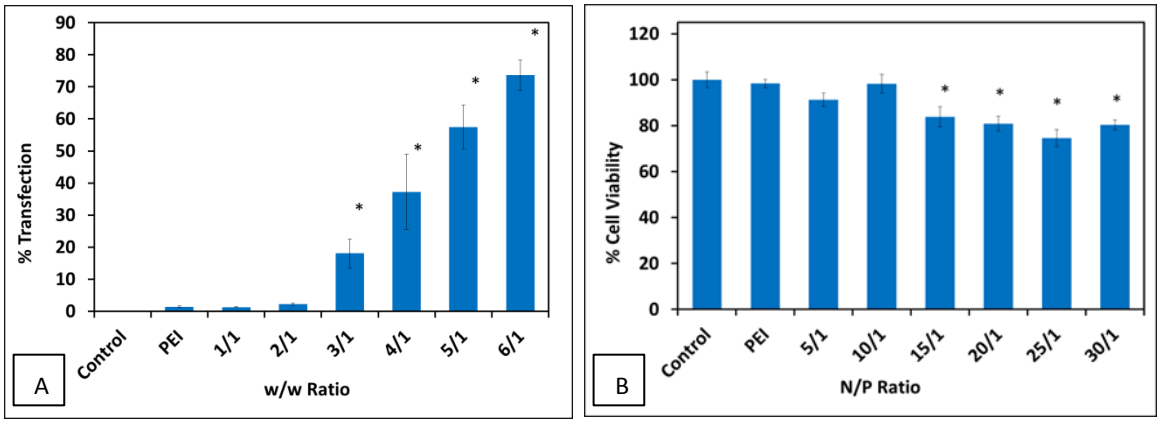

Figure 4.8 C6 cells transfected with PgP-12k-Ab/pGFP in 10% serum; percent transfection (A) and cell viability (B). PEI N/P is 5/1 *:P<0.05 for serum conditions.

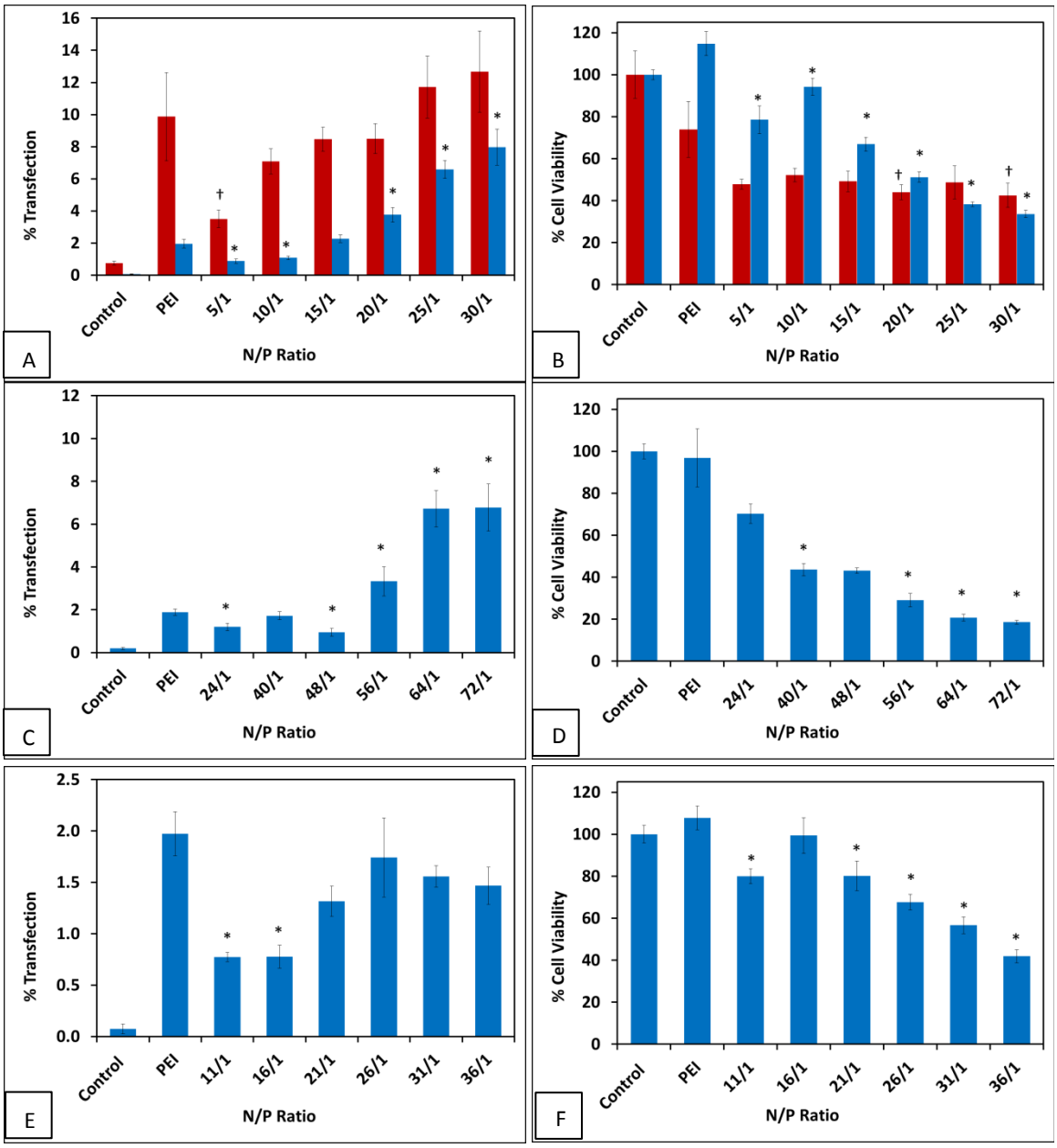

Figure 4.9 CFN cells transfected with PgP-12k/pGFP in 10% serum and non-serum conditions; percent transfection (A) and cell viability (B). CFN cells transfected with PgP-25k/pGFP in 10% serum; percent transfection (C) and cell viability (D). CFN cells transfected with PgP-50k/pGFP in 10% serum; percent transfection (E) and cell viability (F). PEI N/P is 5/1 *:P<0.05 for serum conditions, †:P<0.05 for non-serum compared to PEI

4.4 Generation of Hypoxia as an *in vitro* TBI Model

Western blots done to test for HIF1α in C6 cells showed the highest levels of protein production with 150µM $CoCl_2$ at 24 and 44 hours. (Fig. 4.10A) Beta actin blotting showed equal levels of protein levels (Fig. 4.10B), meaning the change in hypoxia factor was due to hypoxia induction. Neurons were treated with $CoCl_2$ at 100µM and 150µM for 24 hours to test for hypoxia. After staining with betaIII tubulin noticeably less neurite outgrowth was seen. (Fig. 4.11)

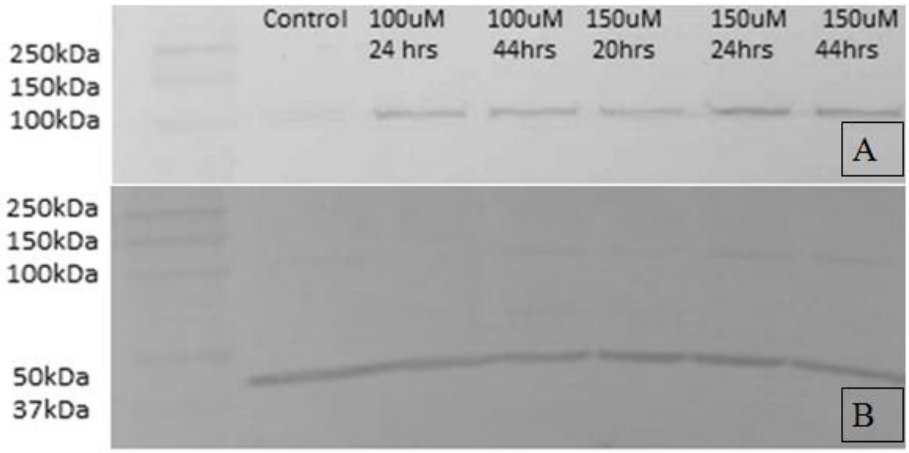

Figure 4.10 Western blot for HIF1α (A) and beta actin (B) from C6 cells treated with $CoCl_2$ to induce hypoxia

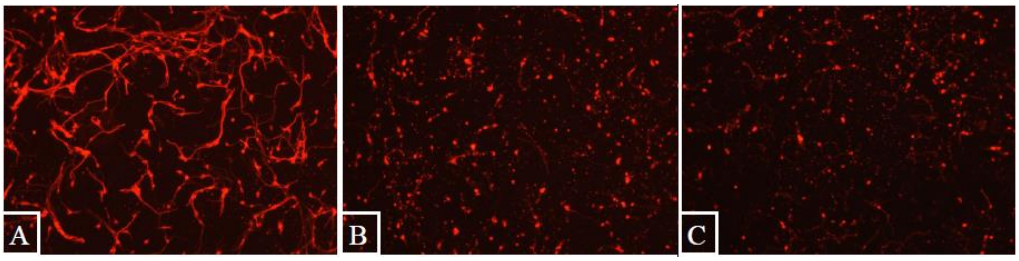

Figure 4.11 Hypoxia on Rat Cerebellar Neurons stained with BetaIII tubulin. No treatment (A), 100µM $CoCl_2$ (B), 150µM $CoCl_2$ (C) for 24 each.

4.5 Rolipram Loading

Rolipram loading was tested by varying rolipram amounts, PgP composition and PgP concentration. PgP-50k at 10mg/mL using 4mg of rolipram was found to be able to load the highest amount rolipram. PgP-50k has the longest hydrophobic portion thus forms a strong hydrophobic core for drug loading (Fig 4.12). Weight of rolipram dissolved was compared with weight of PgP used (Fig. 4.13, primary axis, colored bars). It was found that although higher concentrations of PgP were able to load more rolipram they were not as efficient. This is an important consideration for treatment using rolipram loaded micelles. In order to use rolipram loaded micelles *in vitro* the PgP must be diluted to the concentrations on the order of micrograms. Diluting 10mg/mL PgP to appropriate concentrations would dilute rolipram more than diluting 1mg/mL PgP to appropriate concentrations. Higher rolipram amounts added to PgP solutions showed higher loading amounts. However, higher rolipram amounts were not as efficient as using lower amounts of rolipram. (Fig. 3.13, secondary axis, white bars)

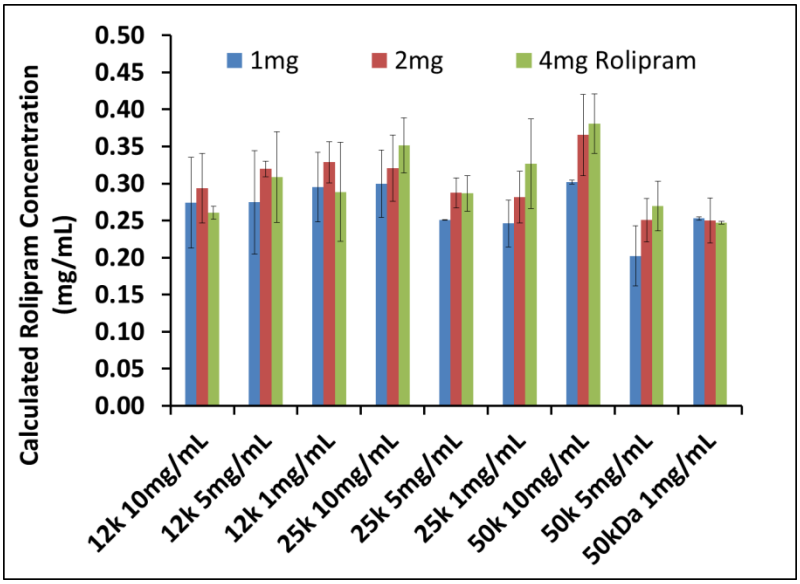

Figure 4.12 PgP loading amounts in PgP-12k, PgP-25k and PgP-50k; each category is amount of rolipram weighed out. Data points are concentration of rolipram dissolved in solution calculated from standard curve by HPLC

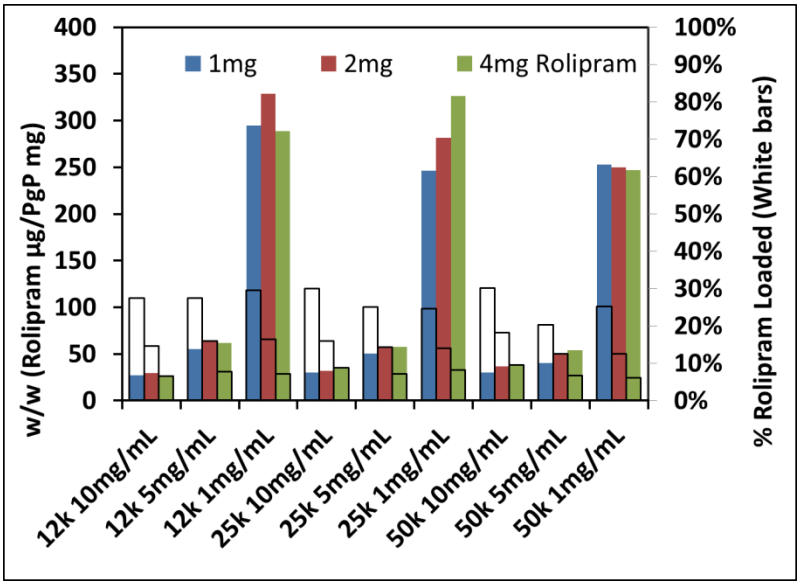

Figure 4.13 Weight/Weight ratio of rolipram loaded by micelle (µg rolipram)/(mg PgP) (colored bars); Percent of dry rolipram used loaded by micelle.

Chapter 5

Conclusion and Future Studies

5.1 Conclusion

The goal of this project was to develop a neuron-specific polymeric micelle nanoparticle delivery system for combinatorial therapy of an siRNA and a drug. This study showed that the PgP micelle is an effective nucleic acid delivery vehicle that can both load drug and conjugate to an antibody. The polymeric micelle was synthesized successfully and important characteristics were measured. Molecular weight and particle size were used to characterize the micelle. Particle size, zeta potential and gel retardation proved stable polyplex formation with pDNA. The critical micelle concentration was calculated. It was also proven that PgP has the ability to conjugate an antibody. This is important because the micelle can be conjugated to anti-NgR1 for neuron specific delivery.

Next, we demonstrated that this PgP micelle is a promising delivery carrier for nucleic acids and drugs in C6 (glioma) cells and primary CFN cells in 10% serum containing medium *in vitro*. The combination of improved transfection and reduced cytotoxicity in the presence of serum relative to conventional b-PEI (25 kDa) control suggest PgP may be a promising nucleic acid carrier for *in vivo* gene delivery. In addition, transfection using PgP-Ab in C6 cells showed that adding an antibody did not hinder transfection efficiency or cytotoxicity.

In addition to showing nucleic acid delivery, hydrophobic drug loading capability of PgP was also demonstrated. The PgP micelle was able to load sufficient amount of

rolipram for treatment of *in vitro* cultured neurons. Lastly, an *in vitro* model for TBI, hypoxia, was generated using cobalt chloride.

5.2 Limitations and Future Studies

PgP molecular weight was calculated using both ^{1}H-NMR and GPC; however, the molecular weight of PgP-50k could not be calculated. We believe this is due to the strong hydrophobic core formed when the polymer is in aqueous solutions interfering with measurements. The next steps for characterization of PgP-50k are to determine an adequate solvent for use in ^{1}H-NMR and GPC.

Transfection in C6 cells was very successful, with both high transfection efficiency and low cytotoxicity. Transfection in CFN showed higher cytotoxicity. The next steps are to use siRNA knockdown to analyze transfection efficacy.

PgP-IgG conjugation was successful. Currently, we are preparing PgP-Ab (Ab:NgR antibody) and evaluating the feasibility of PgP-Ab as a neuron-specific nucleic acid (NgR siRNA) carrier for targeting neuron cells in rat cortical neuron/astrocyte co-culture system. In the future, we will study rolipram-loaded PgP-Ab as a nucleic acid/drug carrier using RhoA siRNA in hypoxia conditions *in vitro* and rat traumatic brain injury model *in vivo*.

Rolipram was successfully loaded into the micelle. The next steps are to determine release of the drug. Using hypoxia as a TBI model, neurons can be treated with free rolipram, rolipram loaded PgP, no treatment and healthy neurons. The cAMP levels of cells can then be analyzed using cAMP ELISA to determine release and effectiveness of rolipram treatments. Finally, an *in vivo* model of traumatic brain injury will be utilized

to test the regenerative capacity of our neuron-targeted, rolipram loaded, RhoA siRNA complexed PgP micelle.

References

[1] Ghajar, J. (2000). Traumatic brain injury. *Lancet*, *356*(9233), 923–9. doi:10.1016/S0140-6736(00)02689-1

[2] "Traumatic Brain Injury." *Centers for Disease Control and Prevention*. Centers for Disease Control and Prevention, 15 Aug. 2013. Web. 18 Nov. 2013. http://www.cdc.gov/TraumaticBrainInjury/index.html

[3] Kelso, M., & Pauly, J. (2011). Therapeutic targets for neuroprotection and/or enhancement of functional recovery following traumatic brain injury. ... *in molecular biology and translational science*, *98*, 85–131. Retrieved from http://ac.els-cdn.com/B978012385506000003X/1-s2.0-B978012385506000003X-main.pdf?_tid=c8191a8d8db9f49cdd0188dc9ae2a963&acdnat=1335675391_0c4f192ae80f0cd4c0b27fb7f197e9be

[4] Schoch, K. M., Madathil, S. K., & Saatman, K. E. (2012). Genetic manipulation of cell death and neuroplasticity pathways in traumatic brain injury. *Neurotherapeutics : the journal of the American Society for Experimental NeuroTherapeutics*, *9*(2), 323–37. doi:10.1007/s13311-012-0107-z

[5] Tong, J., Liu, W., Wang, X., Han, X., Hyrien, O., Samadani, U., … Huang, J. H. (2013). Inhibition of Nogo-66 receptor 1 enhances recovery of cognitive function after traumatic brain injury in mice. *Journal of neurotrauma*, *30*(4), 247–58. doi:10.1089/neu.2012.2493

[6] Akbik, F., Cafferty, W. B. J., & Strittmatter, S. M. (2012). Myelin associated inhibitors: a link between injury-induced and experience-dependent plasticity. *Experimental neurology*, *235*(1), 43–52. doi:10.1016/j.expneurol.2011.06.006

[7] Atkins, C. (2007). Modulation of the cAMP signaling pathway after traumatic brain injury. *Experimental neurology*, *208*(1), 145–158.

[8] Schwab, J. M., Brechtel, K., Mueller, C.-A., Failli, V., Kaps, H.-P., Tuli, S. K., & Schluesener, H. J. (2006). Experimental strategies to promote spinal cord regeneration--an integrative perspective. *Progress in neurobiology*, *78*(2), 91–116. doi:10.1016/j.pneurobio.2005.12.004

[9] Horner, P. J., & Gage, F. H. (2000). Regenerating the damaged central nervous system. *Nature*, *407*, 963–970.

[10] Laabs, T. L., Wang, H., Katagiri, Y., McCann, T., Fawcett, J. W., & Geller, H. M. (2007). Inhibiting glycosaminoglycan chain polymerization decreases the

inhibitory activity of astrocyte-derived chondroitin sulfate proteoglycans. *The Journal of neuroscience : the official journal of the Society for Neuroscience*, *27*(52), 14494–501. doi:10.1523/JNEUROSCI.2807-07.2007

[11] Harris, N. G., Nogueira, M. S. M., Verley, D. R., & Sutton, R. L. (2013). Chondroitinase enhances cortical map plasticity and increases functionally active sprouting axons after brain injury. *Journal of neurotrauma*, *30*(14), 1257–69. doi:10.1089/neu.2012.2737

[12] Chan, C. C. M., Wong, A. K., Liu, J. I. E., Steeves, J. D., & Tetzlaff, W. (2007). ROCK Inhibition with Y27632 Activates Astrocytes and Increases Their Expression of Neurite Growth-Inhibitory Chondroitin Sulfate Proteoglycans, *384*(October 2006), 369–384. doi:10.1002/glia

[13] Fischer, D., He, Z., & Benowitz, L. I. (2004). Counteracting the Nogo receptor enhances optic nerve regeneration if retinal ganglion cells are in an active growth state. *The Journal of neuroscience : the official journal of the Society for Neuroscience*, *24*(7), 1646–51. doi:10.1523/JNEUROSCI.5119-03.2004

[14] Ahmed, Z., Dent, R. G., Suggate, E. L., Barrett, L. B., Seabright, R. J., Berry, M., & Logan, A. (2005). Disinhibition of neurotrophin-induced dorsal root ganglion cell neurite outgrowth on CNS myelin by siRNA-mediated knockdown of NgR, p75NTR and Rho-A. *Molecular and cellular neurosciences*, *28*(3), 509–23. doi:10.1016/j.mcn.2004.11.002

[15] Whitehead, K. a, Langer, R., & Anderson, D. G. (2009). Knocking down barriers: advances in siRNA delivery. *Nature reviews. Drug discovery*, *8*(2), 129–38. doi:10.1038/nrd2742

[16] Partridge, K. a, & Oreffo, R. O. C. (2004). Gene delivery in bone tissue engineering: progress and prospects using viral and nonviral strategies. *Tissue engineering*, *10*(1-2), 295–307. doi:10.1089/107632704322791934

[17] Kreuter, J. (2001). Nanoparticulate systems for brain delivery of drugs. *Advanced drug delivery reviews*, *47*(1), 65–81. Retrieved from http://www.ncbi.nlm.nih.gov/pubmed/11251246

[18] Gao, X., Kim, K.-S., & Liu, D. (2007). Nonviral gene delivery: what we know and what is next. *The AAPS journal*, *9*(1), E92–104. doi:10.1208/aapsj0901009

[19] Nishiyama, N., & Kataoka, K. (2006). Current state, achievements, and future prospects of polymeric micelles as nanocarriers for drug and gene delivery. *Pharmacology & therapeutics*, *112*(3), 630–48. doi:10.1016/j.pharmthera.2006.05.006

[20] Boussif, O., Lezoualc'h, F., Zanta, M. a, Mergny, M. D., Scherman, D., Demeneix, B., & Behr, J. P. (1995). A versatile vector for gene and oligonucleotide transfer into cells in culture and in vivo: polyethylenimine. *Proceedings of the National Academy of Sciences of the United States of America*, *92*(16), 7297–301. Retrieved from http://www.pubmedcentral.nih.gov/articlerender.fcgi?artid=41326&tool=pmcentrez&rendertype=abstract

[21] Cho, Y. W., Kim, J., & Park, K. (2003). Polycation gene delivery systems : escape from endosomes to cytosol, *2003*, 721–734. doi:10.1211/0022357021206

[22] Zhang, C., Gao, S., Jiang, W., Lin, S., Du, F., Li, Z., & Huang, W. (2010). Targeted minicircle DNA delivery using folate-poly(ethylene glycol)-polyethylenimine as non-viral carrier. *Biomaterials*, *31*(23), 6075–86. doi:10.1016/j.biomaterials.2010.04.042

[23] Scholz, C., & Wagner, E. (2012). Therapeutic plasmid DNA versus siRNA delivery: common and different tasks for synthetic carriers. *Journal of controlled release : official journal of the Controlled Release Society*, *161*(2), 554–65. doi:10.1016/j.jconrel.2011.11.014

[24] Misra, A., Ganesh, S., Shahiwala, A., & Shah, S. P. (2003). Drug delivery to the central nervous system: a review. Journal of pharmacy & pharmaceutical sciences : a publication of the Canadian Society for Pharmaceutical Sciences, Société canadienne des sciences pharmaceutiques, 6(2), 252–73. Retrieved from http://www.ncbi.nlm.nih.gov/pubmed/12935438

[25] Margulies, S., & Hicks, R. (2009). Combination therapies for traumatic brain injury: prospective considerations. *Journal of neurotrauma*, *26*(6), 925–39. doi:10.1089/neu.2008-0794

[26] Giger, R. J., Venkatesh, K., Chivatakarn, O., Raiker, S. J., Robak, L., Hofer, T., … Rader, C. (2008). Mechanisms of CNS myelin inhibition: evidence for distinct and neuronal cell type specific receptor systems. *Restorative neurology and neuroscience*, *26*(2-3), 97–115. Retrieved from http://www.ncbi.nlm.nih.gov/pubmed/18820405

[27] GURNEY, MARK. "PDE4 AND TRAUMATIC BRAIN INJURY." (n.d.): n. pag. Web. 29 Dec. 2011. Retrieved from https://tetradiscovery.com/2011/12/new-treatments-for-traumatic-brain-injury/

[28] Lamprecht, a, Ubrich, N., Yamamoto, H., Schäfer, U., Takeuchi, H., Lehr, C.M., … Kawashima, Y. (2001). Design of rolipram-loaded nanoparticles: comparison of two preparation methods. *Journal of controlled release : official journal of the*

Controlled Release Society, *71*(3), 297–306. Retrieved from http://www.ncbi.nlm.nih.gov/pubmed/11295222

[29] Liu, X.-Q., Sun, C.-Y., Yang, X.-Z., & Wang, J. (2013). Polymeric-Micelle-Based Nanomedicine for siRNA Delivery. *Particle & Particle Systems Characterization*, *30*(3), 211–228. doi:10.1002/ppsc.201200061

[30] Anderson, J. M., & Shive, M. S. (2012). Biodegradation and biocompatibility of PLA and PLGA microspheres. *Advanced Drug Delivery Reviews*, *64*, 72–82. doi:10.1016/j.addr.2012.09.004

[31] Pereira, M., & Lai, E. P. (2008). Capillary electrophoresis for the characterization of quantum dots after non-selective or selective bioconjugation with antibodies for immunoassay. *Journal of nanobiotechnology*, *6*, 10. doi:10.1186/1477-3155-6-10

[32] Zhao, Q.-Q., Chen, J.-L., Lv, T.-F., He, C.-X., Tang, G.-P., Liang, W.-Q., … Gao, J.-Q. (2009). N/P ratio significantly influences the transfection efficiency and cytotoxicity of a polyethylenimine/chitosan/DNA complex. *Biological & pharmaceutical bulletin*, *32*(4), 706–10. Retrieved from http://www.ncbi.nlm.nih.gov/pubmed/19336909

[33] Densmore, C. L., Orson, F. M., Xu, B., Kinsey, B. M., Waldrep, J. C., Hua, P., … Knight, V. (2000). Aerosol delivery of robust polyethyleneimine-DNA complexes for gene therapy and genetic immunization. *Molecular therapy : the journal of the American Society of Gene Therapy*, *1*(2), 180–8. doi:10.1006/mthe.1999.0021

[34] Cernak, I. (2005). Animal models of head trauma. *NeuroRx : the journal of the American Society for Experimental NeuroTherapeutics*, *2*(3), 410–22. doi:10.1602/neurorx.2.3.410

[35] Fu, O., Hou, M., & Yang, S. (2009). Cobalt chloride-induced hypoxia modulates the invasive potential and matrix metalloproteinases of primary and metastatic breast cancer cells. *Anticancer …*, *29*, 3131–3138. Retrieved from http://ar.iiarjournals.org/content/29/8/3131.short

[36] Wolfe, C. A., & Hage, D. S. (1995). Studies on the rate and control of antibody oxidation by periodate. *Analytical Biochemistry*, *231*(1), 123–130. Retrieved from http://linkinghub.elsevier.com/retrieve/pii/S0003269785715114

[37] Klegerman, M. E., Hamilton, A. J., Huang, S.-L., Tiukinhoy, S. D., Khan, A. a, MacDonald, R. C., & McPherson, D. D. (2002). Quantitative immunoblot assay for assessment of liposomal antibody conjugation efficiency. *Analytical biochemistry*, *300*(1), 46–52. doi:10.1006/abio.2001.5443

[38] Webb, K., Budko, E., Neuberger, T. J., Chen, S., Schachner, M., & Tresco, P. a. (2001). Substrate-bound human recombinant L1 selectively promotes neuronal attachment and outgrowth in the presence of astrocytes and fibroblasts. *Biomaterials*, *22*(10), 1017–28. Retrieved from http://www.ncbi.nlm.nih.gov/pubmed/11352083

[39] Liang, B., He, M.-L., Xiao, Z.-P., Li, Y., Chan, C.-Y., Kung, H.-F., … Peng, Y. (2008). Synthesis and characterization of folate-PEG-grafted-hyperbranched-PEI for tumor-targeted gene delivery. *Biochemical and biophysical research communications*, *367*(4), 874–80. doi:10.1016/j.bbrc.2008.01.024

[40] Da Cruz, M. T. G., Simões, S., & de Lima, M. C. P. (2004). Improving lipoplex-mediated gene transfer into C6 glioma cells and primary neurons. *Experimental neurology*, *187*(1), 65–75. doi:10.1016/j.expneurol.2003.12.013

[41] Zou, S., Scarfo, K., Nantz, M. H., & Hecker, J. G. (2010). Lipid-mediated delivery of RNA is more efficient than delivery of DNA in non-dividing cells. *International journal of pharmaceutics*, *389*(1-2), 232–43. doi:10.1016/j.ijpharm.2010.01.019

[42] Kievit, F. M., Veiseh, O., Bhattarai, N., Fang, C., Gunn, J. W., Lee, D., … Zhang, M. (2009). PEI-PEG-Chitosan Copolymer Coated Iron Oxide Nanoparticles for Safe Gene Delivery: synthesis, complexation, and transfection. *Advanced Functional Materials*, *19*(14), 2244–2251. doi:10.1002/adfm.200801844

[43] Veiseh, O., Kievit, F. M., Gunn, J. W., Ratner, B. D., & Zhang, M. (2009). A ligand-mediated nanovector for targeted gene delivery and transfection in cancer cells. *Biomaterials*, *30*(4), 649–57. doi:10.1016/j.biomaterials.2008.10.003

[44] Zhang, C., Yadava, P., & Hughes, J. (2004). Polyethylenimine strategies for plasmid delivery to brain-derived cells, *33*, 144–150. doi:10.1016/j.ymeth.2003.11.004